Unraveling Causes for the Changing Behavior of the Tropical Indian Ocean in the Past Few Decades

LEI ZHANG AND WEIQING HAN

Department of Atmospheric and Oceanic Sciences, University of Colorado Boulder, Boulder, Colorado

FRANK SIENZ

Max Planck Institut für Meteorologie, Hamburg, Germany

(Manuscript received 2 July 2017, in final form 7 December 2017)

ABSTRACT

Observations show that decadal (10–20 yr) to interdecadal (>20 yr) variability of the tropical Indian Ocean (TIO) sea surface temperature (SST) closely follows that of the Pacific until the 1960s. Since then, the TIO SST exhibits a persistent warming trend, whereas the Pacific SST shows large-amplitude fluctuations associated with the interdecadal Pacific oscillation (IPO), and the decadal variability of the TIO SST is out of phase with that of the Pacific after around 1980. Here causes for the changing behavior of the TIO SST are explored, by analyzing multiple observational datasets and the recently available large-ensemble simulations from two climate models. It is found that on interdecadal time scales, the persistent TIO warming trend is caused by emergence of anthropogenic warming overcoming internal variability, while the time of emergence occurs much later in the Pacific. On decadal time scales, two major tropical volcanic eruptions occurred in the 1980s and 1990s causing decadal SST cooling over the TIO during which the IPO was in warm phase, yielding the out-of-phase relation. The more evident fingerprints of external forcing in the TIO compared to the Pacific result from the much weaker TIO internal decadal–interdecadal variability, making the TIO prone to the external forcing. These results imply that the ongoing warming and natural external forcing may make the Indian Ocean more active, playing an increasingly important role in affecting regional and global climate.

1. Introduction

Tropical Indian Ocean (TIO) sea surface temperature (SST) plays a crucial role in the Asian summer monsoon system, which has enormous socioeconomic impacts on India and southern Asia (Lau and Waliser 2012) and global climate remotely (Ding and Wang 2005). TIO SST variability is prominently affected by the tropical Pacific (Zhang et al. 1997; Power et al. 1999; Klein et al. 1999). On interannual time scales, El Niño–Southern Oscillation (ENSO) has been shown to cause basinwide warming (during El Niño) and cooling (during La Niña) over the TIO throughout the past century (Klein et al. 1999). On decadal (10–20 yr) to interdecadal (>20 yr) time scales, both observational and numerical modeling studies suggest an in-phase relation between the TIO SST and the interdecadal Pacific oscillation (IPO), the dominant climate mode of the Pacific decadal–interdecadal variability (Zhang et al. 1997; Power et al. 1999).

The atmospheric bridge has been suggested to play an important role in the remote impact of the IPO on TIO SST decadal variability (Deser and Phillips 2006; Copsey et al. 2006; Han et al. 2014a; Dong et al. 2016). In the warm phase of the IPO, anomalous subsidence occurs in the TIO, which reduces local convection and thereby warms the ocean surface; the opposite occurs for the cold IPO phase (Copsey et al. 2006; Dong et al. 2016). Changes in the mixed layer depth and thermocline depth associated with TIO surface wind anomalies induced by the IPO may also contribute to the TIO SST decadal variability (Dong et al. 2016). In addition, the IPO may influence TIO SST through changes in the Indonesian Throughflow (ITF), although such effects may be confined to the southern Indian Ocean (Dong and McPhaden 2016).

Over the past few decades, however, the in-phase relation between the TIO and the IPO breaks down as a

Supplemental information related to this paper is available at the Journals Online website: http://dx.doi.org/10.1175/JCLI-D-17-0445.s1.

Corresponding author: Lei Zhang, lezh8230@colorado.edu

DOI: 10.1175/JCLI-D-17-0445.1

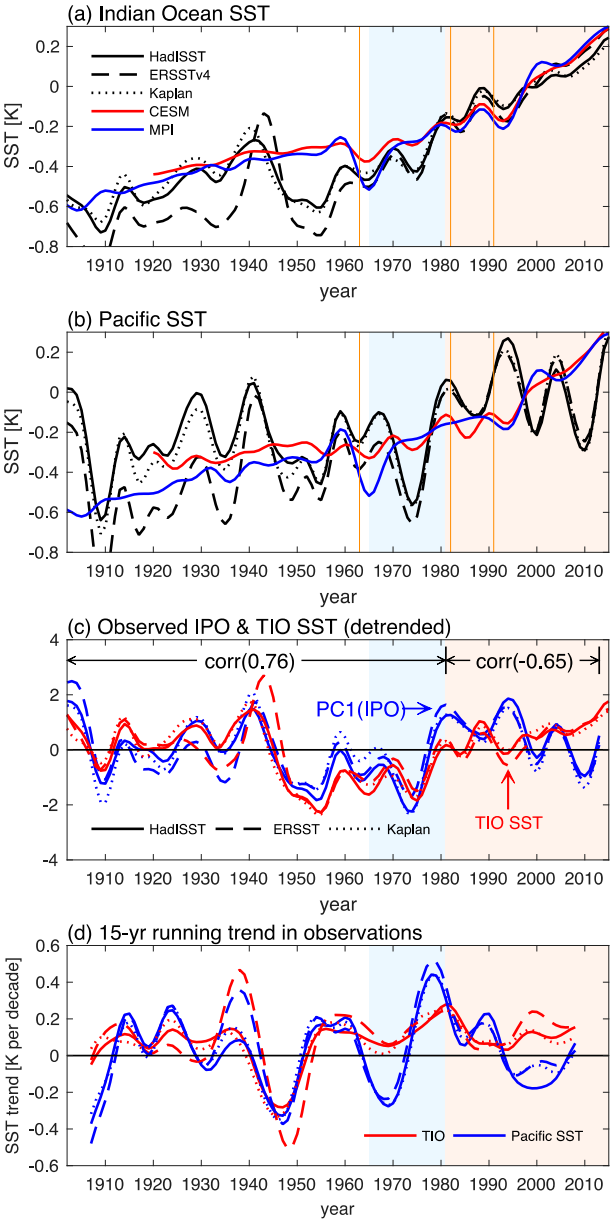

FIG. 1. The 8-yr low-pass-filtered yearly SST anomalies averaged over (a) TIO (20°S–20°N, 50°–90°E) and (b) eastern tropical Pacific (20°S–20°N, 180°–90°W) from observations and ensemble mean of two climate models: CESM (40 members) and the MPI model (100 members). (See boxed regions of Fig. 2.) Anomalies are relative to 1980–2015 averages. Vertical orange lines indicate major tropical volcanic eruptions since 1960s. (c) IPO index (blue) and 8-yr low-pass-filtered, detrended TIO SST index (red) from observational datasets. Both indices are normalized by their respective standard deviation. The average correlation coefficients between the two indices for periods 1902–81 and 1982–2013 from three observational datasets are shown. Since the IPO and the 8-yr low-pass-filtered, detrended eastern tropical Pacific SST index are highly correlated ($r = 0.92$), hereafter we refer the natural decadal variability of the eastern tropical Pacific SST index to as the IPO. (d) The 15-yr running trend of 8-yr low-pass-filtered Indian Ocean (red) and Pacific (blue) SST. Note that the natural variability, which is not synchronous across different ensemble members, has been filtered out in the ensemble mean of CESM and MPI model simulations in (a),(b). Hence, the agreement between ensemble mean results and observations suggests the dominant role of external forcing.

result of the behavioral change of the TIO SST (Han et al. 2014b; Dong and McPhaden 2017). While the Pacific exhibits large-amplitude SST fluctuations associated with the IPO since 1900 (Fig. 1b), the TIO shows a persistent warming trend since the 1960s (Figs. 1a,d), which has been shown to have large impact on the regional and global climate (Giannini et al. 2003; Hoerling et al. 2004), including its impact on the Walker cell and intensified sea level rise in the western tropical Pacific during recent decades (Luo et al. 2012; Han et al. 2014b; Zhang and Karnauskas 2017). On decadal time scales, variability of the TIO and the IPO has been out of phase since around 1980 (correlation of −0.65), contrasting their strong in-phase relationship before around 1980 (correlation of 0.76; Fig. 1c). This suggests that the TIO SST decadal–interdecadal variability no longer follows the IPO during the past few decades.

A recent study (Dong and McPhaden 2017) suggests that even though the IPO entered a negative phase after 2000, it is unable to force a cold TIO because of the TIO warming trend induced by enhanced anthropogenic greenhouse gases during the recent decades through oceanic and atmospheric processes (Du and Xie 2008; Rao et al. 2012; Dong et al. 2014; Han et al. 2014b; Dong and McPhaden 2017); the two effects combine to produce the transformation of the relationship between the IPO and TIO SST in about 1985 (Dong and McPhaden 2017). Despite this progress, causes for the out-of-phase SST relation between the two ocean basins on decadal time scales after around 1980 remain unknown (Fig. 1c). Why the warming trend over the TIO emerges from the SST fluctuations in the 1960s is also not clear.

Understanding the changing behavior of the TIO SST is of paramount importance, because warming over the TIO induced by both external forcing (natural or anthropogenic) and variability internal to the TIO coupled ocean–atmosphere system will intensify convection and thus actively affect the climate in various regions (Deser and Phillips 2006; Annamalai et al. 2007). By contrast, the positive IPO-induced TIO warming will not, because the IPO warms the TIO through increasing atmospheric subsidence and reducing convection, analogous to the impact of ENSO (Kumar and Hoerling 1998; Kumar

et al. 2005; Deser and Phillips 2006; Wu et al. 2006; Copsey et al. 2006; Xie et al. 2009). In this study, we explore causes for the changing behavior of TIO SST variability on decadal and interdecadal time scales, respectively.

2. Data and methods

a. Observational and model data

In this study, we employed the instrumental SST reconstructions for the period 1900–2015 from the Hadley Centre Sea Ice and SST dataset (HadISST; Rayner et al. 2003), the extended-range SST data from the National Oceanic and Atmospheric Administration (NOAA) Extended Reconstructed SST dataset, version 4 (ERSST.v4; Huang et al. 2015), and the Kaplan SST dataset (Kaplan et al. 1998). We also analyzed fully coupled simulations from the National Center for Atmospheric Research (NCAR) Community Earth System Model (CESM) 40-member large ensemble (1920–2100) (Kay et al. 2015) and the Max Planck Institute for Meteorology (MPI) model 100-member large ensemble (1850–2099) (Bittner et al. 2016). The representative concentration pathway 8.5 and 4.5 (RCP8.5 and RCP4.5) forcing scenarios are used in CESM and MPI model future projections (since 2006), respectively. In the RCP8.5 (RCP4.5) experiments, the radiative forcing reaches 8.5 $W m^{-2}$ (4.5 $W m^{-2}$) by the end of the twenty-first century. Although it would be more informative to analyze large-ensemble experiments from the two climate models using same forcing scenario, only large-ensemble CESM simulations with the RCP8.5 scenario and MPI model with the RCP4.5 scenario are available for analysis currently. It is also worth mentioning that the current generation of climate models still have some critical problems in reproducing mean-state SST, especially in the tropical Pacific (e.g., cold tongue bias), which may affect both simulated SST natural variability and projected SST response to external forcing. This is a caveat that one needs to bear in mind when interpreting our results.

b. Methods

To obtain the IPO-related SST variability, we conducted empirical orthogonal function (EOF) analysis. Zhang (2016) pointed out that the first two leading EOF modes of the 5-yr running mean global yearly SST essentially describe the anthropogenic global warming mode (EOF1) and the IPO (EOF2), respectively. The 5-yr running mean filter was applied to remove the ENSO influence. Interested readers can refer to Zhang (2016) for a more in-depth discussion. Here, we first removed the ensemble mean yearly SST from each ensemble member for both CESM and MPI model to remove the externally forced signals (primarily anthropogenic warming trend), then we conducted EOF analysis of the 8-yr low-pass-filtered global yearly SST. The 5-yr running mean filter and 8-yr low-pass filter generate very similar results. For observational SST datasets, we removed the long-term linear warming trend grid by grid prior to conducting the EOF analysis. The resulting leading EOF mode describes the IPO (Fig. 2). Patterns of the linear SST warming trend from observations and the ensemble mean of the two models are shown in Fig. 3.

In this study, we define the Pacific SST index as the SST averaged over the eastern tropical Pacific (20°S–20°N, 180°–90°W) to describe the IPO (Fig. 2). The correlation coefficient between the natural decadal variability of the eastern tropical Pacific SST index and the corresponding principal component of the EOF1 mode (PC1) is 0.94 (0.9) in CESM (MPI model) on average and 0.93 in observations (see Fig. S1 in the supplemental material). We also calculated the tripole index for the IPO from NOAA (https://www.esrl.noaa.gov/psd/data/timeseries/IPOTPI/), and found that the correlation coefficient between the natural decadal variability of the two indices is 0.95 (0.94) in CESM (MPI model), and 0.91 in observations. Hence, we refer to the natural decadal variability of the eastern tropical Pacific SST index as the IPO in this study. We also define an Indian Ocean SST index as SST averaged over the region 20°S–20°N, 50°–90°E. Results are not sensitive to the choice of the region (Fig. S2 in the supplemental material). To obtain the natural decadal variability of the Indian Ocean and Pacific SST indices in the two models, we first removed the ensemble mean values and then applied an 8-yr low-pass Butterworth filter to the SST indices.

3. Results

a. IPO and anthropogenic warming in observations and climate models

To explore causes for the changing behavior of the TIO SST variability, we analyze multiple observational datasets and the recently available large-ensemble simulations from two state-of-the-art global climate models, the CESM (40-member ensemble) and the MPI model (100-member ensemble). The large-ensemble simulation is a useful tool to isolate externally forced signals and internal variability of the climate system, because the internal variability is not synchronous across individual realizations and the ensemble-mean approach effectively suppresses the internal variability and isolates effects of the external forcing (both natural and anthropogenic forcing).

We first evaluate the simulation of the IPO in the two climate models by comparing it with the observations,

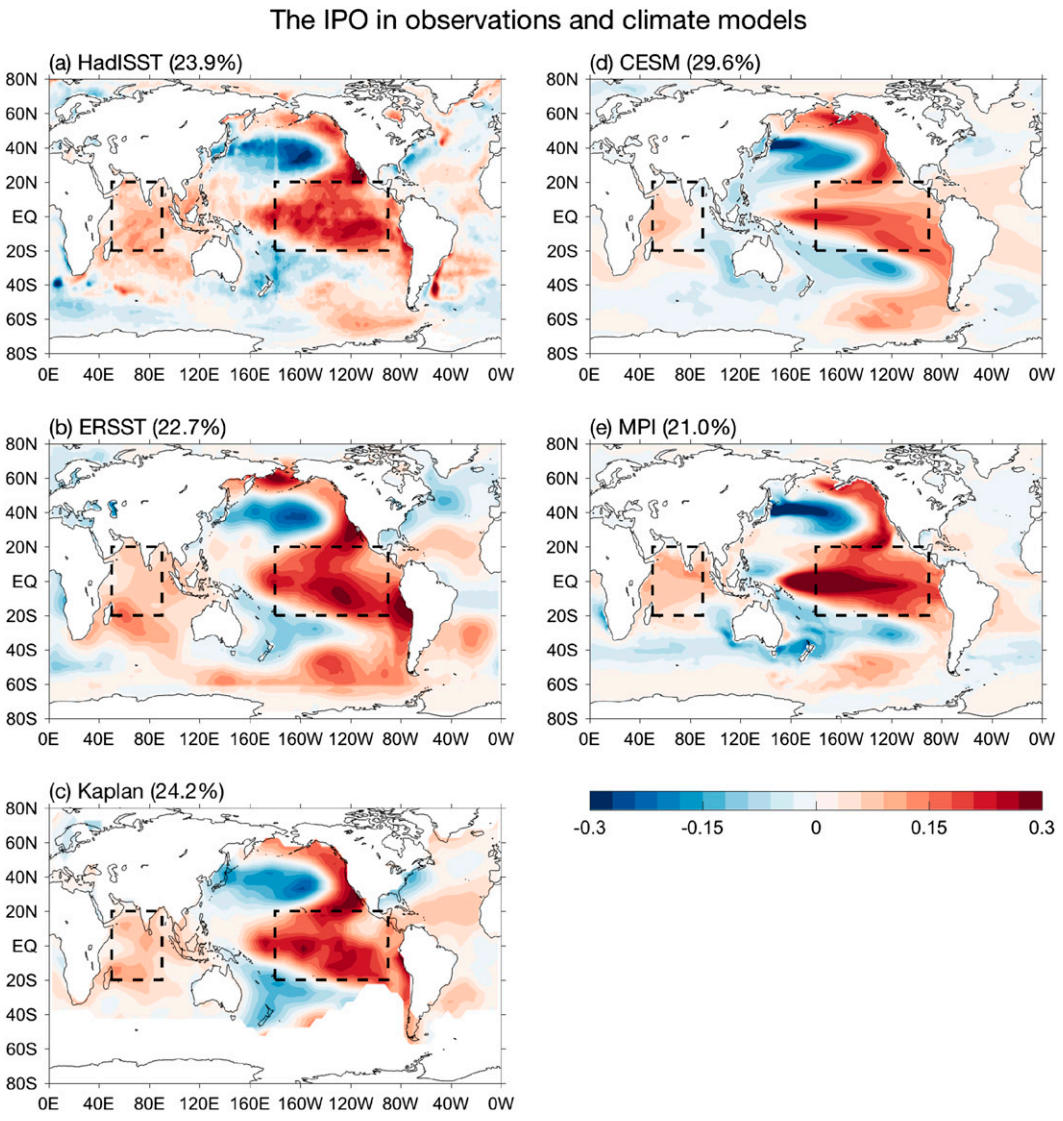

FIG. 2. The EOF1 of 8-yr low-pass-filtered global yearly SST from observational datasets and two climate models. Anthropogenic warming signals were removed prior to conducting the EOF analysis. Results are shown for (a) HadISST, (b) ERSST.v4, and (c) Kaplan SST datasets for the 1900–2015 period and (d) the 40-member average of EOF1 for CESM (1920–2005) and (e) 100-member average of EOF1 for the MPI model (1850–2005). Variance explained by the EOF1 mode is shown in parentheses in each panel. Dashed boxes in (a)–(e) denote the regions for calculating the SST indices.

because the natural decadal–interdecadal variability of the TIO SST is closely connected with the IPO (Krishnan and Sugi 2003; Han et al. 2014a). We find that the IPO-related SST anomaly pattern is very similar between observations and climate models, which exhibit a meridional tripolelike SST anomaly pattern prevailing in the Pacific (Fig. 2). The TIO SST anomaly associated with the IPO is in phase with that over the eastern tropical Pacific, with a much smaller amplitude over the TIO compared to the Pacific. Natural decadal variability of the TIO and the IPO are highly correlated in the two models, particularly the MPI model, as found in observations (Fig. 4b).

However, there are some noticeable discrepancies between the model simulations and observations. In particular, the IPO-related SST anomalies over the TIO manifest as an Indian Ocean dipole (IOD)-like pattern in models (Figs. 2d,e), contrasting the basinwide SST anomalies in observations (Figs. 2a–c). This discrepancy may be related to the larger variance of SST over the southeast Indian Ocean in climate models compared to observations (Deser et al. 2012; Weller and

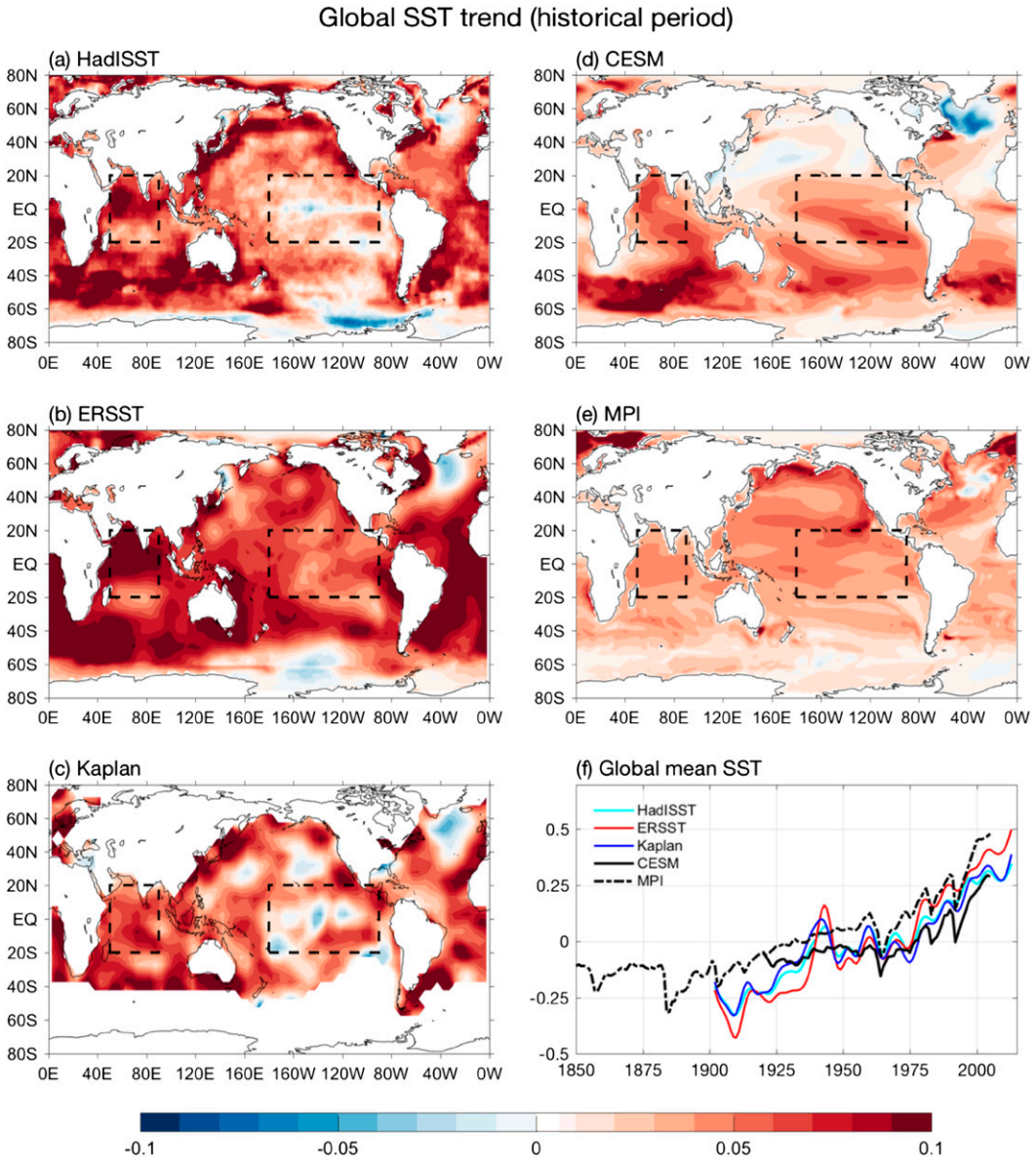

FIG. 3. The spatial pattern of linear SST trend (K decade^{-1}) from (a) HadISST, (b) ERSST.v4, and (c) Kaplan SST datasets for the period 1900–2015. The SST trend (K decade^{-1}) from the ensemble mean of (d) CESM (1920–2005) and (e) the MPI model (1850–2005). (f) The time evolution of 8-yr low-pass-filtered global mean SST from observational datasets and ensemble mean of the two climate models; mean values are removed.

Cai 2013; Cai and Cowan 2013). Nevertheless, it is clear that the IPO-related SST variability is reasonably simulated by the two models.

On the other hand, although the evolution of global mean SST is reasonably simulated in the two climate models, the pattern of anthropogenic warming trends exhibit large discrepancies between observations and climate models (Fig. 3), particularly for the tropical Pacific, which has been noted in previous studies (Zhang and Li 2014; Zhang 2016). The distinctions among the results for the three observational datasets and the two climate models are also noticeable. This could be associated with the sparse observations during the early twentieth century (Deser et al. 2010) and/or model deficiency. We note that there are large SST fluctuations in the tropical Pacific associated with the IPO throughout the twentieth century (Fig. 1b), which may also contribute to the large uncertainty in the linear SST warming trend pattern in the tropical Pacific. In the TIO, the warming trend is overall weaker in models compared with observations, which may also be associated with the interference of the evident natural variability prior to the

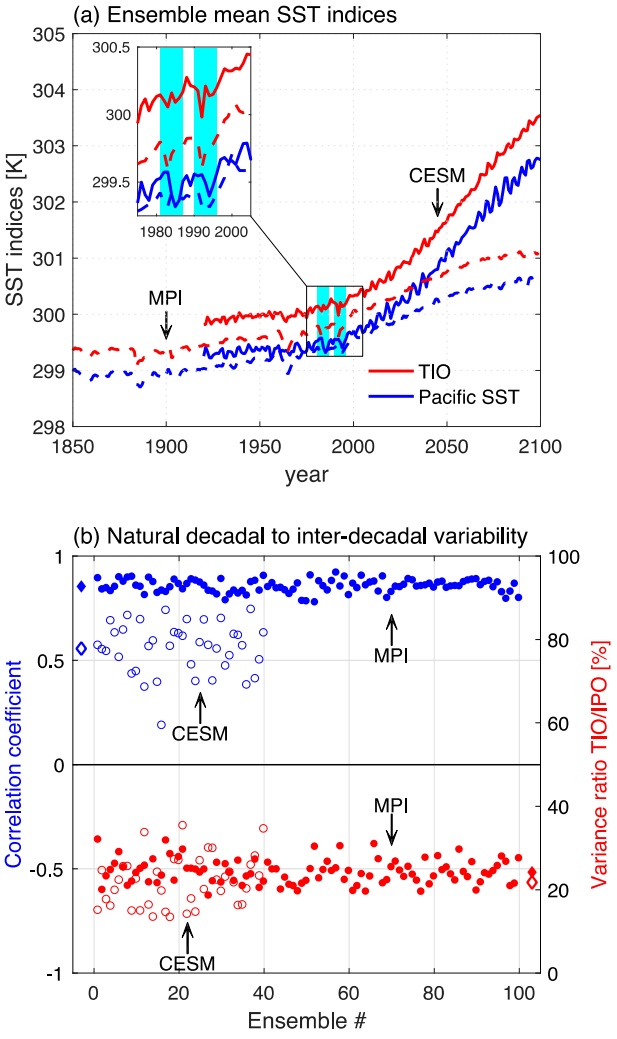

FIG. 4. (a) Time evolution of ensemble mean SST indices (solid for CESM; dashed for the MPI model), which assess the external (natural plus anthropogenic) forcing. We zoom in to show the impact of volcanic forcing in the 1980s and 1990s (inset). (b) Correlation coefficients between natural internal variability of the two SST indices (left *y* axis, blue circles) and variance ratio between the two indices (right *y* axis, red circles) in the MPI model (filled) and CESM (open). Diamonds denote the ensemble mean values. Note the leveling off of the SST warming trend in the MPI model after around 2050 in (a), which is associated with the slowdown of the increasing rate of the radiative forcing in the RCP4.5 future scenario used in the MPI model. In CESM, RCP8.5 scenario is used, and thus the warming magnitude is greater in CESM than in the MPI model during the twenty-first century.

1960s (Fig. 1a), which is filtered out in the ensemble mean results of the two models.

b. Decadal variability of Indian Ocean SST

To assess the relative importance of external forcing and internal natural variability in SST variability in the tropical Indo-Pacific region, the ensemble mean of the two models, which isolates the effects of natural plus anthropogenic external forcing, is compared against observations (Figs. 1a,b). If the ensemble mean result agrees with the observations, it suggests that the external forcing plays a dominant role. Note that natural variability in different ensemble members of CESM and MPI model simulations is not synchronous, and natural variability in these models does not correspond to actual events in observations. For instance, the ensemble mean result do not capture the recent global warming hiatus after around 2000 (Figs. 1a,b), which has been attributed to the negative phase of the IPO (Kosaka and Xie 2013; England et al. 2014).

The ensemble-mean TIO SST variability in CESM and MPI model agrees well with observations after around 1960, successfully capturing both the persistent warming trend and the decadal variability during the 1980s and 1990s, suggesting a dominant role of external forcing during this period (Fig. 1a). Prior to the 1960s, the observed TIO SST variability is clearly dominated by the IPO, which is filtered out by the ensemble-mean approach in models (Figs. 1a,c). The Pacific SST variability, on the other hand, exhibits large model/data discrepancy throughout the historical period (Fig. 1b); while the Pacific SST exhibits large-amplitude fluctuations associated with the IPO in observations, the ensemble-mean Pacific SST from climate models shows a steady warming trend. Hence, these results suggest that the changing behavior of the TIO SST over the past few decades mainly arises from the external forcing, which has much less impact on the Pacific SST variability associated with the IPO.

How does the external forcing cause TIO SST variability on decadal time scales? The external forcing mostly comes from the anthropogenic greenhouse gases, especially for future projections. However, this forcing induces a relatively steady warming trend in both Indian and Pacific Oceans, in contrast with the evident TIO SST cooling followed by quick recoveries in the 1980s and 1990s in the ensemble mean of both models (Figs. 1a,b). Hence, the TIO SST decadal variability is unlikely caused by greenhouse gases. The SST decrease is not due to anthropogenic aerosols either, which would cause SST cooling with a much smoother curve at a much longer time scale. Note that the timing of the observed and simulated ensemble mean TIO SST decreases in the early 1980s and early 1990s coincides with two major tropical volcanic eruptions—El Chichón (1982) and Mount Pinatubo (1991) (Santer et al. 2014)—which exert negative radiative forcing over the TIO and cause SST reduction. We indeed find large negative surface solar radiation anomalies over the tropical Indo-Pacific region corresponding to major tropical volcanic eruptions

(Fig. S3 in the supplemental material). Hence, the TIO SST decadal variability during the 1980s and 1990s is primarily caused by tropical volcanic eruptions. Meanwhile, the IPO was in warm phase during 1980–2000, yielding the out-of-phase relationship between the IPO and TIO SST since around 1980. While the TIO SST recovers from the eruption of El Chichón in the late 1980s, the IPO index decreases. This opposite change of the IPO is likely part of its internal variability, which can be enhanced by the warm TIO intensifying Pacific trade winds and therefore increasing oceanic upwelling (Luo et al. 2012; Han et al. 2014b; Zhang and Karnauskas 2017). After around 2000, the TIO SST shows a positive trend resulting from increased anthropogenic greenhouse gases, while the IPO transits to a negative phase (Dong and McPhaden 2017). Impact of the volcanic forcing on TIO SST is also visible in the 1960s (Mount Agung), but it overlies a weak negative IPO phase (Figs. 1a–c). Hence, the TIO SST decrease in the 1960s is likely contributed by both external forcing (volcanoes) and natural variability (IPO), and consequently, the IPO and TIO SST remain in phase.

Why does the natural external forcing by volcanoes have such a predominant effect on the TIO but little effect on the Pacific SST? As noted above, the TIO natural decadal variability tends to follow the IPO, but the amplitudes of decadal SST fluctuations are much smaller over the TIO than the Pacific (Figs. 1a,b and 2). Variance of the internal variability (with externally forced signals removed) of the TIO SST on decadal–interdecadal time scales is only 21% of that for the IPO in CESM and 25% in the MPI model for all ensemble members (Figs. 4b and 5a). In contrast, the external forcing induces SST anomalies of similar amplitudes over the two basins (Fig. 5a), and therefore, the externally forced signal to natural internal variability (noise) ratio over the TIO is around 5 times of that over the Pacific. For instance, variance of the externally forced SST variability is approximately 11 times that of the internal variability over the TIO but only approximately 2.3 times that of the IPO after around 2050 in CESM (Fig. 5a). Consequently, the weak natural decadal variability in the TIO makes the external forcing more evident compared with the Pacific; thus, the TIO decadal variability is more easily overwhelmed by the externally forced signals.

c. *Indian Ocean SST warming trend*

Because of the relatively short lifetime, the effect of the volcanic forcing primarily affects the TIO SST decadal variability (Fig. 1a). On interdecadal time scales, weak natural variability also makes the TIO more vulnerable to the long-lived anthropogenic greenhouse

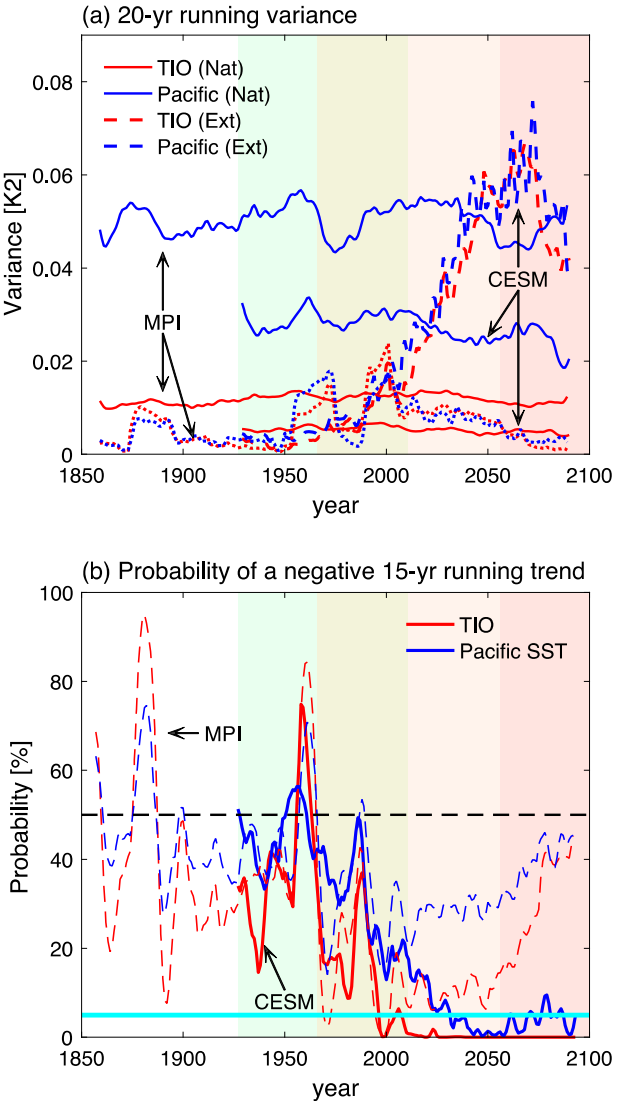

FIG. 5. (a) Ensemble mean 20-yr running variance (K^2) of externally forced and internal components of the SST indices. (b) Probability of a negative 15-yr trend in the 8-yr low-pass-filtered SST indices in CESM (solid) and the MPI model (dashed). The x axis is the centered year of the 15-yr trend. Black dashed (cyan solid) line denotes the 50% (5%) level.

gases. The increased greenhouse gases cause a steady upward SST trend over the TIO and the Pacific (Fig. 4a). While the warming trend dominates interdecadal fluctuations over the TIO during recent decades, Pacific SST fluctuations remain large because of the dominance of the IPO (Figs. 1a,b). Note that the decadal cooling in the 1980s and 1990s associated with the volcanic forcing does not affect the overall multidecadal warming trend over the TIO after around 1960 (Fig. 1d).

To quantify the relative importance of the anthropogenic warming trend and natural variability (IPO) in

determining the TIO SST interdecadal variability, we show the time evolution of the probability of a cooling trend over the TIO and the Pacific, evaluated using all the ensemble members of the two climate models (Fig. 5b). Note that the probability of a cooling trend would be approximately 50% if there is no external forcing (perfectly randomly distributed IPO phase); however, because of the anthropogenic warming trend, the probability of an interdecadal cooling trend will decrease and eventually become highly unlikely. Indeed, we find that prior to the mid-1960s, the externally forced SST variability is weak, and the probability of a cooling and warming 15-yr SST trend is almost equal on average for both the TIO and the Pacific (Fig. 5b). After the mid-1960s, the anthropogenic warming rate evidently increases (Figs. 1a,b and 4a), resulting in a sudden drop in the probability of a cooling trend over the TIO. This downward tendency continues as anthropogenic warming increases, and the occurrence of a cooling trend over the TIO becomes extremely unlikely (probability $< 5\%$) after around 2000 in CESM (Fig. 5b). In comparison, a decrease in the probability of a Pacific SST cooling trend is clearly slower, thanks to strong SST fluctuations associated with the IPO that interfere with the anthropogenic warming. As a result, a cooling trend over the Pacific becomes extremely unlikely ($<5\%$) after around 2040, which is approximately 40 years later than the TIO. This result is consistent with observations (Fig. 1); time of emergence, the time when anthropogenic warming trend emerges from natural variability (the time after which the probability of a cooling trend remains less than 5%), occurs much earlier in the TIO than the Pacific. Note that this time of emergence perspective has considered the impact of the IPO, but it does not depend on the model IPO phase. This result suggests that in the future, the anthropogenic warming trend will slowly dominate over the natural variability (the IPO), and as a result, even when there is a negative IPO that may cause a cooling trend, the actual trend (anthropogenic warming trend plus negative IPO) will still be positive. Also note that there are abrupt rises in the probability of a cooling trend in the 1960s and 1980s in both basins, which is associated with volcanic forcing during these periods (Zhang 2016; Kosaka and Xie 2016). It is also worth noting that the tropical volcanic eruptions in the 1980s and 1990s may cause a delay in the time of emergence of the TIO warming trend (Fig. 5b).

The MPI model shows similar results to CESM for the historical period. For the future projection, the MPI model exhibits a recovery of the probability of a cooling trend after around 2050 for both the Pacific and the TIO (Fig. 5b). This is because the MPI model used the less aggressive radiative forcing scenario (RCP4.5) whereas CESM used the business-as-usual RCP8.5 scenario. As a result, the anthropogenic SST warming trend is smaller and levels off after around 2050 in the MPI model compared to CESM (Fig. 5a), and tropical oceans become slowly dominated by the natural variability again in the MPI model's future projection. The prominent discrepancy between the two models implies the importance of a climate change mitigation policy.

To demonstrate the changing behavior of TIO SST during different temporal periods, we show the probability density function (PDF) of a 15-yr SST trend for the periods pre-1965, post-1965, near future, and late twenty-first century (Fig. 6). The PDF shifts to a higher positive value from early twentieth century to the near future in both basins as a result of the anthropogenic greenhouse gas effect in both models. More importantly, the probability of a TIO cooling trend during the post-1965 period drops to approximately one-third of that for the pre-1965 period (Figs. 6a,c), whereas it only decreases somewhat for the Pacific in the two models (Figs. 6b,d). These model results agree qualitatively with observations (Figs. 6e,f), despite some differences likely due to the small sample size of observations. These results clearly demonstrate the dominant role of the anthropogenic greenhouse gas effect in the TIO SST variability during the historical period, whereas decadal SST cooling associated with the IPO strongly acts against the anthropogenic warming in the Pacific. In CESM, the probability of a TIO cooling trend becomes negligible during the late twenty-first century, while there remains a small chance ($\sim 2\%$) for a tropical Pacific cooling trend (Figs. 6a,b). In contrast, the PDFs in the MPI model reverse back in both TIO and the Pacific after the mid-twenty-first century (Figs. 6c,d), because of its RCP4.5 scenario that requires a strong policy to curb the greenhouse gases' emission.

To show which region of the tropical oceans is more prone to the anthropogenic warming, we obtain spatial patterns of the time of emergence across the tropical oceans in the climate model (Fig. 7). Given that the TIO SST interdecadal variability is dominated by the natural internal variability in late twenty-first century in the MPI model (Fig. 5b), we only show the CESM results. Large SST fluctuations over the eastern tropical Pacific associated with the IPO make this region less vulnerable to the anthropogenic warming, yielding a rather late time of emergence. Note that the probability of an eastern Pacific surface cooling trend cannot be entirely discarded even until the end of this century with the "business as usual" forcing scenario. Given that the tropical Pacific SST plays a crucial role in determining the evolution of global mean surface temperature (Kosaka and Xie 2013), our result suggests that the global warming hiatus may reoccur in the future. In contrast, the relatively weak

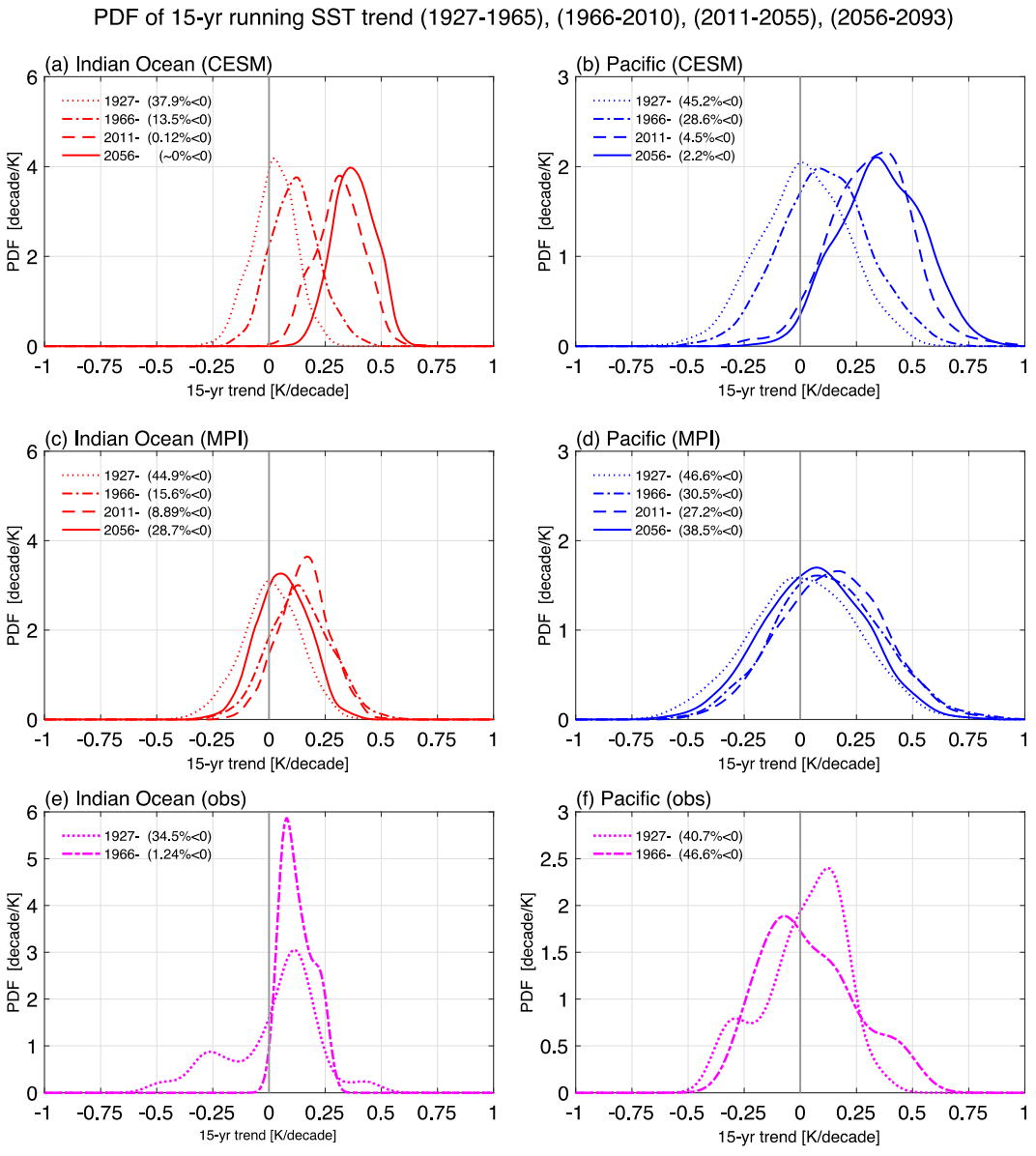

FIG. 6. PDF of the 15-yr running trend of (left) 8-yr low-pass-filtered TIO SST index and (right) the IPO index in models and observational datasets. PDFs are evaluated for the four periods: pre-1965 (1927–65; dotted), post-1965 (1966–2010; dotted–dashed), near future (2011–55; dashed), and second half of the twenty-first century (2056–93; solid) for (a),(b) CESM, (c),(d) the MPI model, and (e),(f) observations. Probability of a negative SST trend is shown in parentheses in each panel.. All three observational SST datasets employed in this study were used to calculate the PDF in (e),(f).

decadal variability in the TIO makes this region much more easily overwhelmed by external forcings, which results in a much earlier time of emergence of the anthropogenic warming trend. Note that the time of emergence is relatively early in the tropical Atlantic as well. Thus, the time of emergence map agrees with the observed interbasin warming contrast over the recent decades (i.e., prominent SST warming trends over the TIO and tropical Atlantic), while the SST warming trend in the tropical Pacific is relatively small and uncertain (Luo et al. 2012; McGregor et al. 2014; Zhang and Karnauskas 2017).

4. Summary and discussion

Natural decadal (10–20 yr) to interdecadal (>20 yr) variability of the tropical Indian Ocean (TIO) SST is primarily forced by the IPO, and hence, the TIO SST and the IPO exhibit a strong in-phase relation. This

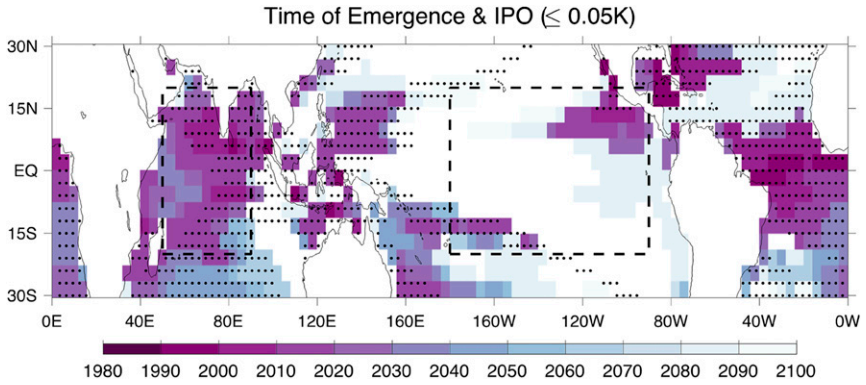

FIG. 7. The years after which the probability of a negative 15-yr trend of 8-yr low-pass-filtered SST remains less than 10% until the end of the twenty-first century in CESM. The probability is evaluated at a 4° × 4° grid cell. Stippling denotes the regions where amplitude of the IPO-related SST anomalies is equal to or smaller than 0.05 K (Fig. 2d).

passive behavior of the Indian Ocean, however, has changed in the past few decades; while the TIO exhibits a persistent warming trend after the 1960s, Pacific SST shows large fluctuations associated with the IPO; the decadal variability of the TIO SST is opposite to that over the Pacific since around 1980. Causes for the changing behavior of the TIO SST variability on both decadal and interdecadal time scales are investigated.

Analysis of the large-ensemble simulations from CESM and MPI model reveals that external forcings from both tropical volcanic eruptions and anthropogenic greenhouse gases are crucial for the observed changing behavior of the TIO SST. While the volcanic forcing induces the Indian Ocean decadal (10–20 yr) SST cooling during the 1980s and 1990s, the IPO was in a positive phase, yielding the out-of-phase relation between the two basins. The interdecadal SST warming trend in the TIO since around 1960 is associated with the emergence of an anthropogenic warming trend overcoming the natural variability associated with the IPO influence. In contrast, the time of emergence of the anthropogenic warming signals in the Pacific is much later (~2040 with CESM results). As a result, the observed TIO SST exhibits a persistent warming trend accompanying large Pacific SST fluctuations associated with the IPO since 1960. Note that the focus of this study is on the decadal–interdecadal variability of the TIO SST and its relationship with the Pacific. On the interannual time scale, ENSO plays an important role in modulating the Indian Ocean SST variability (Klein et al. 1999) even after the 1980s (Fig. 3 of Han et al. 2014b).

The more evident fingerprints of external forcings (both natural and anthropogenic) in the Indian Ocean compared to the Pacific result from the much weaker Indian Ocean natural decadal–interdecadal variability. The externally forced signal-to-noise (internal variability) ratio in the TIO is approximately 5 times of that in the Pacific, which makes the Indian Ocean more prone to the external forcing. Both the changing behavior of the Indian Ocean SST and its underlying causes are robust to cross-dataset and cross-model differences.

A recent study by Dong and McPhaden (2017) found that the changing relation between the TIO SST variability and the IPO at the interdecadal time scale is largely attributed to anthropogenic greenhouse gases causing Indian Ocean warming, while the IPO was in a negative phase, similar to our findings here. However, this study further explores the cause for the out-of-phase relation between the Indian and Pacific Oceans at a decadal (10–20 yr) time scale particularly since the 1980s, which is attributable to volcanic forcing. Furthermore, we explain the reason from the time of emergence perspective, showing that the Indian Ocean exhibits persistent warming while the IPO exhibits large oscillations in recent decades, which yields their out-of-phase relation at the interdecadal time scale.

Results present in this study imply that the ongoing warming and natural external forcing play a dominant role in determining the Indian Ocean SST decadal–interdecadal variability, which will make the Indian Ocean more "active," instead of just passively controlled by the Pacific. Indeed, the recent Indian Ocean warming trend has been shown to play an important role in enhancing the eastern Pacific surface cooling trend, and thus actively contributes to the recent global warming hiatus (Luo et al. 2012; Han et al. 2014b; Zhang and Karnauskas 2017). It is also worth mentioning that some recent studies have linked the Indian Ocean warming trend to the ENSO impact through the atmospheric bridge (Roxy et al. 2014). The IPO is also shown to prominently modulate the Indian Ocean heat content through the ITF (Lee et al. 2015; Li et al. 2017). These observational studies suggest an important role of the Pacific in the

Indian Ocean decadal–interdecadal variability. A recent study (Li et al. 2016) suggests that the Indian Ocean warming in the past few decades may be primarily caused by the Atlantic warming. Here we show that the Indian Ocean warming trend is attributable to the early time of emergence of the anthropogenic warming trend. Hence, our work implies that the Indian Ocean may play an active role in affecting climate over the Pacific and other regions, rather than being just a passive receiver from other ocean basins, given that the mean SST is high (>28°C) in most regions of the tropical Indian Ocean. Future studies targeting the impact of Indian Ocean SST variability on other tropical ocean basins using delicately designed numerical experiments are needed.

Acknowledgments. We thank Dr. Jochem Marotzke for providing the MPI large-ensemble simulations and Luis Kornblueh, Jürgen Kröger, and Michael Botzet for performing the MPI model experiments. The CESM Large Ensemble Community Project and supercomputing resources were provided by NSF/CISL/Yellowstone. L. Z. and W. H. are supported by NSF Grant AGS-1446480.

REFERENCES

Annamalai, H., H. Okajima, and M. Watanabe, 2007: Possible impact of the Indian Ocean SST on the Northern Hemisphere circulation during El Niño. *J. Climate*, **20**, 3164–3189, https://doi.org/10.1175/JCLI4156.1.

Bittner, M., H. Schmidt, C. Timmreck, and F. Sienz, 2016: Using a large ensemble of simulations to assess the Northern Hemisphere stratospheric dynamical response to tropical volcanic eruptions and its uncertainty. *Geophys. Res. Lett.*, **43**, 9324–9332, https://doi.org/10.1002/2016GL070587.

Cai, W., and T. Cowan, 2013: Why is the amplitude of the Indian Ocean dipole overly large in CMIP3 and CMIP5 climate models? *Geophys. Res. Lett.*, **40**, 1200–1205, https://doi.org/10.1002/grl.50208.

Copsey, D., R. Sutton, and J. R. Knight, 2006: Recent trends in sea level pressure in the Indian Ocean region. *Geophys. Res. Lett.*, **33**, L19712, https://doi.org/10.1029/2006GL027175.

Deser, C., and A. S. Phillips, 2006: Simulation of the 1976/77 climate transition over the North Pacific: Sensitivity to tropical forcing. *J. Climate*, **19**, 6170–6180, https://doi.org/10.1175/JCLI3963.1.

——, ——, and M. A. Alexander, 2010: Twentieth century tropical sea surface temperature trends revisited. *Geophys. Res. Lett.*, **37**, L10701, https://doi.org/10.1029/2010GL043321.

——, and Coauthors, 2012: ENSO and Pacific decadal variability in the Community Climate System Model version 4. *J. Climate*, **25**, 2622–2651, https://doi.org/10.1175/JCLI-D-11-00301.1.

Ding, Q., and B. Wang, 2005: Circumglobal teleconnection in the Northern Hemisphere summer. *J. Climate*, **18**, 3483–3505, https://doi.org/10.1175/JCLI3473.1.

Dong, L., and M. J. McPhaden, 2016: Interhemispheric SST gradient trends in the Indian Ocean prior to and during the recent global warming hiatus. *J. Climate*, **29**, 9077–9095, https://doi.org/10.1175/JCLI-D-16-0130.1.

——, and ——, 2017: Why has the relationship between Indian and Pacific Ocean decadal variability changed in recent decades? *J. Climate*, **30**, 1971–1983, https://doi.org/10.1175/JCLI-D-16-0313.1.

——, T. Zhou, and B. Wu, 2014: Indian Ocean warming during 1958–2004 simulated by a climate system model and its mechanism. *Climate Dyn.*, **42**, 203–217, https://doi.org/10.1007/s00382-013-1722-z.

——, ——, A. Dai, F. Song, B. Wu, and X. Chen, 2016: The footprint of the inter-decadal Pacific oscillation in Indian Ocean sea surface temperatures. *Sci. Rep.*, **6**, 21251, https://doi.org/10.1038/srep21251.

Du, Y., and S.-P. Xie, 2008: Role of atmospheric adjustments in the tropical Indian Ocean warming during the 20th century in climate models. *Geophys. Res. Lett.*, **35**, L08712, https://doi.org/10.1029/2008GL033631.

England, M. H., and Coauthors, 2014: Recent intensification of wind-driven circulation in the Pacific and the ongoing warming hiatus. *Nat. Climate Change*, **4**, 222–227, https://doi.org/10.1038/nclimate2106.

Giannini, A., R. Saravanan, and P. Chang, 2003: Oceanic forcing of Sahel rainfall on interannual to interdecadal time scales. *Science*, **302**, 1027–1030, https://doi.org/10.1126/science.1089357.

Han, W., J. Vialard, M. J. McPhaden, T. Lee, Y. Masumoto, M. Feng, and W. P. M. de Ruijter, 2014a: Indian Ocean decadal variability: A review. *Bull. Amer. Meteor. Soc.*, **95**, 1679–1703, https://doi.org/10.1175/BAMS-D-13-00028.1.

——, and Coauthors, 2014b: Intensification of decadal and multi-decadal sea level variability in the western tropical Pacific during recent decades. *Climate Dyn.*, **43**, 1357–1379, https://doi.org/10.1007/s00382-013-1951-1.

Hoerling, M. P., J. W. Hurrell, T. Xu, G. T. Bates, and A. S. Phillips, 2004: Twentieth century North Atlantic climate change. Part II: Understanding the effect of Indian Ocean warming. *Climate Dyn.*, **23**, 391–405, https://doi.org/10.1007/s00382-004-0433-x.

Huang, B., and Coauthors, 2015: Extended Reconstructed Sea Surface Temperature version 4 (ERSST.v4). Part I: Upgrades and intercomparisons. *J. Climate*, **28**, 911–930, https://doi.org/10.1175/JCLI-D-14-00006.1.

Kaplan, A., M. A. Cane, Y. Kushnir, A. C. Clement, M. B. Blumenthal, and B. Rajagopalan, 1998: Analyses of global sea surface temperature 1856–1991. *J. Geophys. Res.*, **103**, 18 567–18 589, https://doi.org/10.1029/97JC01736.

Kay, J. E., and Coauthors, 2015: The Community Earth System Model (CESM) Large Ensemble project: A community resource for studying climate change in the presence of internal climate variability. *Bull. Amer. Meteor. Soc.*, **96**, 1333–1349, https://doi.org/10.1175/BAMS-D-13-00255.1.

Klein, S. A., B. J. Soden, and N.-C. Lau, 1999: Remote sea surface temperature variations during ENSO: Evidence for a tropical atmospheric bridge. *J. Climate*, **12**, 917–932, https://doi.org/10.1175/1520-0442(1999)012<0917:RSSTVD>2.0.CO;2.

Kosaka, Y., and S.-P. Xie, 2013: Recent global-warming hiatus tied to equatorial Pacific surface cooling. *Nature*, **501**, 403–407, https://doi.org/10.1038/nature12534.

——, and ——, 2016: The tropical Pacific as a key pacemaker of the variable rates of global warming. *Nat. Geosci.*, **9**, 669–673, https://doi.org/10.1038/ngeo2770.

Krishnan, R., and M. Sugi, 2003: Pacific decadal oscillation and variability of the Indian summer monsoon rainfall. *Climate Dyn.*, **21**, 233–242, https://doi.org/10.1007/s00382-003-0330-8.

Kumar, A., and M. P. Hoerling, 1998: Specification of regional sea surface temperatures in atmospheric general circulation

model simulations. *J. Geophys. Res.*, **103**, 8901–8907, https://doi.org/10.1029/98JD00427.

Kumar, K. K., M. P. Hoerling, and B. Rajagopalan, 2005: Advancing dynamical prediction of Indian monsoon rainfall. *Geophys. Res. Lett.*, **32**, L08704, https://doi.org/10.1029/2004GL021979.

Lau, W. K.-M., and D. E. Waliser, 2012: *Intraseasonal Variability in the Atmosphere–Ocean Climate System*. 2nd ed. Springer, 614 pp.

Lee, S.-K., W. Park, M. O. Baringer, A. L. Gordon, B. Huber, and Y. Liu, 2015: Pacific origin of the abrupt increase in Indian Ocean heat content during the warming hiatus. *Nat. Geosci.*, **8**, 445–449, https://doi.org/10.1038/ngeo2438.

Li, X., S.-P. Xie, S. T. Gille, and C. Yoo, 2016: Atlantic-induced pan-tropical climate change over the past three decades. *Nat. Climate Change*, **6**, 275–279, https://doi.org/10.1038/nclimate2840.

Li, Y., W. Han, and L. Zhang, 2017: Enhanced decadal warming of the southeast Indian Ocean during the recent global surface warming slowdown. *Geophys. Res. Lett.*, **44**, 9876–9884, https://doi.org/10.1002/2017GL075050.

Luo, J.-J., W. Sasaki, and Y. Masumoto, 2012: Indian Ocean warming modulates Pacific climate change. *Proc. Natl. Acad. Sci. USA*, **109**, 18 701–18 706, https://doi.org/10.1073/pnas.1210239109.

McGregor, S., A. Timmermann, M. F. Stuecker, M. H. England, M. Merrifield, F.-F. Jin, and Y. Chikamoto, 2014: Recent Walker circulation strengthening and Pacific cooling amplified by Atlantic warming. *Nat. Climate Change*, **4**, 888–892, https://doi.org/10.1038/nclimate2330.

Power, S., T. Casey, C. Folland, A. Colman, and V. Mehta, 1999: Inter-decadal modulation of the impact of ENSO on Australia. *Climate Dyn.*, **15**, 319–324, https://doi.org/10.1007/s003820050284.

Rao, S. A., A. R. Dhakate, S. K. Saha, S. Mahapatra, H. S. Chaudhari, S. Pokhrel, and S. K. Sahu, 2012: Why is Indian Ocean warming consistently? *Climatic Change*, **110**, 709–719, https://doi.org/10.1007/s10584-011-0121-x.

Rayner, N. A., D. E. Parker, E. B. Horton, C. K. Folland, L. V. Alexander, D. P. Rowell, E. C. Kent, and A. Kaplan, 2003: Global analyses of sea surface temperature, sea ice, and night marine air temperature since the late nineteenth century. *J. Geophys. Res.*, **108**, 4407, https://doi.org/10.1029/2002JD002670.

Roxy, M. K., K. Ritika, P. Terray, and S. Masson, 2014: The curious case of Indian Ocean warming. *J. Climate*, **27**, 8501–8509, https://doi.org/10.1175/JCLI-D-14-00471.1.

Santer, B. D., and Coauthors, 2014: Volcanic contribution to decadal changes in tropospheric temperature. *Nat. Geosci.*, **7**, 185–189, https://doi.org/10.1038/ngeo2098.

Weller, E., and W. Cai, 2013: Realism of the Indian Ocean dipole in CMIP5 models: The implications for climate projections. *J. Climate*, **26**, 6649–6659, https://doi.org/10.1175/JCLI-D-12-00807.1.

Wu, R., B. P. Kirtman, and K. Pegion, 2006: Local air–sea relationship in observations and model simulations. *J. Climate*, **19**, 4914–4932, https://doi.org/10.1175/JCLI3904.1.

Xie, S.-P., K. Hu, J. Hafner, H. Tokinaga, Y. Du, G. Huang, and T. Sampe, 2009: Indian Ocean capacitor effect on Indo–western Pacific climate during the summer following El Niño. *J. Climate*, **22**, 730–747, https://doi.org/10.1175/2008JCLI2544.1.

Zhang, L., 2016: The roles of external forcing and natural variability in global warming hiatuses. *Climate Dyn.*, **47**, 3157–3169, https://doi.org/10.1007/s00382-016-3018-6.

——, and T. Li, 2014: A simple analytical model for understanding the formation of sea surface temperature patterns under global warming. *J. Climate*, **27**, 8413–8421, https://doi.org/10.1175/JCLI-D-14-00346.1.

——, and K. B. Karnauskas, 2017: The role of tropical interbasin SST gradients in forcing Walker circulation trends. *J. Climate*, **30**, 499–508, https://doi.org/10.1175/JCLI-D-16-0349.1.

Zhang, Y., J. M. Wallace, and D. S. Battisti, 1997: ENSO-like interdecadal variability: 1900–93. *J. Climate*, **10**, 1004–1020, https://doi.org/10.1175/1520-0442(1997)010<1004:ELIV>2.0.CO;2.